Altered Expression of Glomerular Heat Shock Protein 27 in Experimental Nephrotic Syndrome

William E. Smoyer,* Avneesh Gupta,* Peter Mundel,‡ Jeffrey D. Ballew,§ and Michael J. Welsh§

*Departments of *Pediatrics and Anatomy and §Cell Biology, University of Michigan, Ann Arbor, Michigan 48109; and ‡Department of Anatomy and Cell Biology I, University of Heidelberg, Heidelberg, Germany*

Abstract

Although nephrotic syndrome is a very common kidney disease, little is known about the molecular changes occurring within glomerular capillary loops during development of disease. The characteristic histologic change is retraction (effacement) of the distal "foot" processes of glomerular epithelial cells (GEC) which surround the capillary loops. The GEC foot processes are an essential part of the kidney's filtration barrier, and their structure is regulated primarily by actin microfilaments, cytoskeletal proteins present in high concentrations in foot processes. Actin polymerization has been reported to be regulated via phosphorylation of the low molecular weight heat shock protein, hsp27. We localized hsp27 within normal rat GECs using immunofluorescence and immunoelectron microscopy. Induction of nephrotic syndrome and GEC foot process effacement using the puromycin aminonucleoside rat model resulted in significant increases in: (*a*) renal cortical hsp27 mRNA expression (826±233%, x±SEM, $P < 0.01$ vs. control); (*b*) glomerular hsp27 protein expression (87±2%, $P < 0.001$ vs. control); and (*c*) glomerular hsp27 phosphorylation (101±32%, $P < 0.05$ vs. control). These findings support the hypothesis that hsp27, by regulating GEC foot process actin polymerization, may be important in maintaining normal foot process structure, and regulating pathophysiologic GEC cytoskeletal changes during development of nephrotic syndrome. (*J. Clin. Invest.* 1996. 97:2697–2704.) Key words: nephrotic syndrome • heat shock proteins • hsp27 • actin • puromycin aminonucleoside

Introduction

Nephrotic syndrome is among the most common forms of kidney disease seen in children, with an estimated incidence of 2–7 new cases per 100,000 children annually (1). It is characterized clinically by the development of massive proteinuria, hypoalbuminemia, and edema. In health, one of the most important functions of the kidneys is to maintain the body's fluid balance by filtering the blood, allowing excretion of appropriate amounts of fluid while retaining the cells and most proteins within the bloodstream. In nephrotic syndrome, the kidney's filtration barrier is altered in such a way that massive amounts of protein are lost in the urine. The resulting low oncotic pressure in the blood permits fluid to leak from the bloodstream into the surrounding tissues causing edema throughout the body (2). Despite extensive studies in humans (3–9) and a well-established rat model of nephrotic syndrome (puromycin aminonucleoside nephrosis [PAN])[1] (10–14), the pathogenesis of this disease remains unclear. Although it is generally suspected that unidentified circulating factor(s), possibly cytokines, are responsible for the actual pathophysiologic changes in the kidney (15, 16), an unknown initiating event(s) ultimately leads to a critical alteration in the physical structure of the filtration barrier within the kidney's filtering unit, the glomerulus. Using electron microscopy (EM), this alteration is characterized by retraction and widening (effacement) of the distal "foot" processes of the glomerular epithelial cells (GEC) which surround each of the capillary loops in the glomerulus (17). Progressive effacement of these processes results in the formation of a nearly continuous cytoplasmic sheet covering the glomerular capillary wall. This GEC structural alteration, often associated with detachment from the underlying glomerular basement membrane (GBM), has been shown to correlate closely with the development of proteinuria (10, 11, 18) and is the characteristic ultrastructural finding for the nephrotic syndrome.

In recent immunofluorescence (IF) staining studies, we have discovered the presence of the low molecular weight heat shock protein (hsp), hsp27, in normal rat kidneys which is localized specifically to the site of the glomerular filtration barrier (capillary loop). Glomerular capillary loops are comprised of endothelial cells, GBM, and GECs whose distal foot processes are known to contain high concentrations of the cytoskeletal protein actin (19, 20). Although hsp27 may be expressed in endothelial cells, recent reports demonstrating that hsp27 can regulate actin polymerization in vitro (21–23) and that it may associate with actin microfilaments in some cells (M.J. Welsh, W. Wu, M. Parvinen, R.R. Gilmont, manuscript submitted for publication), combined with its pattern of localization, suggested that glomerular capillary loop hsp27 may be expressed primarily, or exclusively, in GECs. Taken together, these findings led us to hypothesize that hsp27 may play an important role in the maintenance of the kidney's normal filtration barrier, possibly via regulation of actin microfilament dynamics in GEC foot processes.

The potential involvement of hsp27 in maintaining the kidney's normal filtration barrier suggested that this molecule might also play a role in the development of kidney disease in

Address correspondence to William E. Smoyer, M.D., Pediatric Nephrology, University of Michigan Medical Center, Box 0684, 7510 MSRB I, 1150 W. Medical Center Drive, Ann Arbor, MI 48109. Phone: 313-763-9524; FAX: 313-936-7083; E-mail: william.smoyer@umich.edu

Received for publication 29 September 1995 and accepted in revised form 22 March 1996.

J. Clin. Invest.

0021-9738/96/06/2697/08 $2.00
Volume 97, Number 12, June 1996, 2697–2704

1. *Abbreviations used in this paper:* EM, electron microscopy; GBM, glomerular basement membrane; GEC, glomerular epithelial cell; hsp, heat shock protein; IF, immunofluorescence; PAN, puromycin aminonucleoside nephrosis.

which there were significant structural alterations of the filtration barrier. The nephrotic syndrome was felt to be the ideal disease to study this question, as it is characterized by marked effacement of the GEC foot processes comprising the kidney's filtration barrier. More importantly, in animal models of the nephrotic syndrome, alterations in GEC structure have been shown to be closely linked to actin disaggregation and an altered distribution of actin filaments within the GEC (24–26). In the most established animal model of nephrotic syndrome, 3–7 d after treatment with a single dose of PAN rats develop proteinuria, ascites, and effacement of GEC foot processes which histologically resembles human nephrotic syndrome (27). In an attempt to test our hypothesis that hsp27 may play a role in the development of GEC foot process effacement and nephrotic syndrome, we studied the expression and phosphorylation of glomerular hsp27 during development of experimental nephrotic syndrome in normal rats.

Methods

Experimental model

Animals and induction of nephrotic syndrome. Experiments were performed using 50 adult male Sprague-Dawley rats (175–200 grams). Rats were obtained from the specific pathogen-free breeding colony of the Laboratory Animal Core of the National Institutes of Health P30 Center for the Study of Reproduction at the University of Michigan. Nephrotic syndrome was induced in 25 animals by a single intraperitoneal injection of PAN (150 mg/kg), while 25 matched control animals received equal intraperitoneal volumes of normal saline. Each animal was housed in an individual metabolic cage to allow for collection of urine and was given free access to water and standard rat chow. Serial 24-h urine samples were collected from each animal just prior to PAN injection and 1, 3, 7, and 10 d after injection for measurement of proteinuria. Matched control and diseased animals were sacrificed at 0.5, 1, 3, 7, and 10 d after injection. The kidneys were harvested, rinsed in cold PBS, and the renal capsules removed. Glomeruli were isolated from one kidney from each animal by mincing cortical tissue with a razor blade, rinsing with cold PBS, pressing the tissue through a No. 140 stainless steel sieve (W.S. Tyler, Mentor, OH) wetted with cold PBS and collecting the glomeruli on a No. 200 sieve, as previously described by Kreisberg et al. (28). After rinsing again with cold PBS, glomeruli were counted under the microscope, and the procedure repeated until each sample had > 95% glomeruli. The remaining kidney was hemisected, the cortex isolated from one of the hemisections, and the tissue snap frozen in liquid nitrogen and stored at −80°C for subsequent RNA isolation. The other hemisected section was prepared as follows. (*a*) one cortical fraction was cut into 1-mm cubes and fixed in 4% gluteraldehyde/0.1 M cacodylate buffer for EM evaluation; and (*b*) one fraction was placed in OCT solution (Tissue-Tek, Elkhart, IN) on a glass slide and frozen at −80°C for later cryosectioning for IF evaluation.

Clinical confirmation of disease. All 24-h urine specimens were analyzed for total protein using precipitation in 30% TCA on ice for 60 min. Precipitated proteins were resuspended in 0.25 N NaOH and the protein concentrations determined using Coomassie Protein Assay Reagent (Pierce, Rockford, IL) with spectrophotometric analysis at 595 nm and comparison to known albumin standards also diluted in 0.25 N NaOH.

Histologic confirmation of changes in GEC foot process structure. All animals were evaluated by EM for confirmation of development of the GEC foot process effacement which is characteristic of the nephrotic syndrome. Samples were fixed overnight in 4% gluteraldehyde in 0.1 M cacodylate buffer, washed, and postfixed in 2% OsO_4 in 0.1 M cacodylate buffer. After repeat washing in buffer, samples were dehydrated with graded ethanol solutions and propylene oxide, infiltrated with graded Epon:propylene oxide solutions, embedded in pure Epon, and baked overnight at 65°C. Thin sections were then cut and mounted on nickel grids, and evaluated for GEC foot process effacement by transmission EM.

Glomerular hsp27 protein expression

IF staining. Tissues frozen in OCT solution were cut in 4-μm sections, placed on polylysine-coated glass slides, and stored at −80°C until stained. Sections to be stained were thawed and fixed for 5 min in acetone at room temperature. After washing in PBS × 3, samples were blocked with 10% goat/10% rat serum in PBS × 15 min, rinsed in PBS × 3 again and incubated with a 1:100 dilution of ascites fluid of mouse anti-hsp27 monoclonal antibody for 45 min at room temperature. This monoclonal antibody was generated against a 15 amino acid synthetic peptide (residues 123–137) derived from the highly conserved C-terminal domain of human hsp27, and its specificity for hsp27 has been previously described by Bitar et al. (29). After washing in PBS, samples were incubated with FITC-labeled polyclonal goat anti-mouse IgG (Cappel, Organon Teknika Corp., West Chester, PA) diluted 1:50 in blocking serum solution for 30 min. The samples were then washed in PBS × 3, the coverslips mounted with *N*-propyl gallate, and stored at 4°C in a light-proof container.

Semi-quantitative confocal microscopy. Estimation of relative amounts of glomerular hsp27 by IF was performed on 1 micron thick optical section images generated from kidney sections (stained as above) using a Bio-Rad MC600 laser-scanning confocal microscope. Images from 10 randomly selected glomeruli from each animal were analyzed pixel-by-pixel to determine the average fluorescence value per pixel (range 0–256 U) of each individual glomerulus. The average fluorescence values per pixel from the ten glomeruli from each animal were then averaged to yield glomerular brightness values for each animal. Average glomerular brightness values from all matched control animals were combined, and represent the mean of 25 animals, or 250 glomeruli. Similar values for PAN-treated animals at each time point represent the mean of 5 animals, or 50 glomeruli. For all optical brightness measurements, all settings of the confocal microscope and laser system were held constant.

Isoelectric focusing gel electrophoresis and analysis. Glomerular proteins from glomeruli isolated from each animal were solubilized in a buffer consisting of 2% NP-40 (Sigma Chemical Co., St. Louis, MO), 9 M urea and 0.002% β-mercaptoethanol for 1 h at 37°C. Samples were centrifuged at 12,000 *g* for 10 min, and protein concentrations of the supernatants were determined by spectrophotometry using a commercially available colorimetric protein assay kit (Coomassie Protein Assay Reagent, Pierce, Rockford, IL) with albumin standards prepared in solubilization buffer. The isoelectric focusing gels consisted of 5.8% acrylamide, 0.2% bis-acrylamide, 2.5% pH 4-6 ampholyte (Serva, Heidelberg, Germany), 2.5% pH 5-8 ampholyte (Sigma Chemical Co.), 5% glycerol and 6 M urea, polymerized with 0.015% ammonium persulfate, 0.0005% riboflavin 5′-phosphate and 0.03% TEMED, and 0.4-mm thick gels were cast for use in a mini-isoelectric focusing cell (Bio-Rad Model 111, Hercules, CA). 20 μg of glomerular protein from each animal was then loaded into each lane. Gels were run for 15 min at 100 V, 15 min at 250 V and at least 60 min at 450 V, transferred to Whatman 3 MM filter paper by direct contact, and the protein electroblotted onto PVDF membranes (Millipore, Bedford, MA) for 1 hr at 70 mA in transfer buffer containing 0.0375% SDS, 39 mM glycine, and 48 mM Tris. Membranes were then stained for total protein with a solution containing 50% methanol, 0.1% Coomassie brilliant blue R-250 (Sigma Chemical Co.), and 7% acetic acid for 5 min, partially destained with 50% methanol and 7% acetic acid, and rinsed with ddH_20. Computer images of the membranes were scanned and relative protein loading between lanes quantitated using the NIH Image 1.56 computer program for normalization of hsp27 protein expression results. Each previously stained membrane was then blocked with 5% nonfat milk in PBS/0.1% Tween 20 (PBS-T) for 1 h at room temperature, incubated with anti-hsp27 mAb in blocking solution for 1 h, and washed 3 × 10 min in

PBS-T. After this, blots were incubated with a polyclonal donkey anti–mouse IgG conjugated to horseradish peroxidase (Jackson ImmunoResearch Laboratories, West Grove, PA) in blocking solution for 1 h, the peroxidase was activated for fluorescence emission using an enhanced chemiluminescence kit (Amersham, Arlington Heights, IL), and the blots exposed to x-ray film. To optimize densitometric readings for each of the hsp27 isoforms, blots were analyzed after two different exposure times. The resultant unphosphorylated and phosphorylated hsp27 isoform bands were quantitated with densitometry using the NIH Image 1.56 program. Paired control and PAN-treated total protein values (from the above Coomassie stained membranes) for each time point were then used to normalize hsp27 results based on relative protein loading.

Renal cortical hsp27 mRNA expression

RNA isolation. Total RNA was extracted from hemisected kidney cortex sections from each animal using the RNA Stat-60 kit (Tel-Test, Friendswood, TX). Each tissue was thawed, minced and rinsed free of blood with sterile PBS. Minced tissue was combined with 1.0 ml RNA Stat-60 and homogenized. After five minutes 200 μl chloroform was added and each sample was vortexed vigorously and then centrifuged for 15 min at 12,000 *g* at 4°C. The aqueous phase was retrieved, combined with 500 μl isopropanol, and precipitated at −80°C for 15 min. The tube was centrifuged at 12,000 *g* for 10 min at 4°C and the RNA pellet washed with 75% ethanol and centrifuged again. Each pellet was partially dried at 37°C and dissolved in DEPC-treated H_20. RNA yield and purity were estimated spectrophotometrically by absorbance at 260 and 280 nm.

Northern blotting. Total RNA (80 μg/sample) was run on 1.0% agarose gels containing 6.1% formaldehyde, blotted onto Hybond N+ nylon membranes (Amersham, Arlington Heights, IL) by capillary transfer, and fixed to the membranes with a UV cross-linker, using a standard protocol (30). Insert containing rat hsp27 cDNA (0.8 kb) (R.R. Gilmont and M.J. Welsh. 1992. Expression of HSP27 mRNA in the postnatal rat testis. Accession No. M86389, NCBI gi: 204664) was extracted from pBluescript (Stratagene, La Jolla, CA) using EcoRI restriction sites in the polycloning region of the plasmid, and the cDNA isolated using low melting point agarose electrophoresis (BRL, Gaithersburg, MD). The hsp27 cDNA probe was labeled with α-^{32}P-dCTP using a commercially available random priming kit (Random Primers DNA Labeling System, BRL, Gaithersburg, MD), and separated from unincorporated ^{32}P-dNTPs using a Sephadex G-50 spin column (Sigma Chemical Co.). Blots were prehybridized for 2 hours at 42°C, denatured radiolabeled probe was added with fresh hybridization solution, and the blots were hybridized overnight at 42°C. Blots were washed 4 times and then exposed to x-ray film for 2–5 d in a cassette containing intensifying screens. Resulting autoradiographs were analyzed by densitometry using the NIH Image 1.56 image analysis program. All values were normalized for RNA loading by densitometric analysis of EtBr-stained 18s rRNA bands in each gel prior to transfer.

Immunoelectron microscopy

Kidney cortex from normal adult Sprague-Dawley rats was prepared for analysis by perfusion-fixation with 2% paraformaldehyde, then further fixation of small pieces of cortex for 1 h in the same fixative, and cryoprotection for 2 h in 1.725 M sucrose and 25% polyvinylpyrrolidone in PBS. The tissue was mounted on aluminum nails and frozen in liquid nitrogen. Ultrathin (50–100 nm) frozen sections were then cut at −110°C on a Reichert Ultracut E equipped with the cryoattachment FC 4E. The sections were transferred to formvar-coated nickel grids (100 mesh) and stored overnight at 4°C on 2% gelatin before immunolabeling.

Grids were incubated by floating on drops of filtered solutions in a moist chamber. After washing with PBS, nonspecific binding sites were blocked for 1 h at room temperature with 10% fetal calf serum (FCS) containing 10 mM glycine to block free aldehyde groups. Grids were incubated at 4°C overnight with a 1:100 dilution of the hsp27 mAb, rinsed with 0.1% BSA in PBS, then incubated for 1 hour at room temperature with a 1:50 dilution of rabbit anti-mouse IgG (Zymed, Aidenbach, FRG) in 10% FCS in PBS as a bridge, followed by a goat anti–rabbit IgG coupled to 10 nm colloidal gold (Biocell, Plano, Marburg, FRG) at a 1:100 dilution in PBS containing 0.1% acetylated BSA to reduce nonspecific absorption of the gold-labeled antibody to the formvar film. The grids were then rinsed 10 times in 0.1% BSA in PBS and twice in PBS, postfixed with 2% gluteraldehyde (Merck, Darmstadt, FRG) for 10 min, and stained with either 2% OsO_4, 1% reduced OsO_4, or 1% tannic acid followed by 2% OsO_4. After staining with 2% uranyl acetate for 2–5 min, they were finally absorption-stained with 0.003% lead citrate in 2% polyvinyl alcohol, dried at room temperature, and observed using a Phillips EM 301 electron microscope.

Statistics

All data are expressed as the mean±SEM. All statistics were performed using unpaired, two-tailed *t* tests to compare results from control animals to PAN-treated animals. Results were considered statistically significant if $P < 0.05$, and represent data collected from five independent experiments, each with five control and five PAN-treated animals.

Results

PAN nephrosis

Clinical confirmation of disease. Fig. 1 shows the resultant 24-h proteinuria over the 10 d after PAN injection. Significant proteinuria developed by day 7 and increased markedly by day 10 ($x = 506 \pm 96$ mg/24 h, $P < 0.001$ vs. control), as has been previously reported (18).

Histologic confirmation of changes in GEC foot process structure. Evaluation of kidney sections by EM revealed that, during the 10 d after PAN treatment, all animals treated with PAN developed diffuse effacement of GEC foot processes compared with controls. A representative comparison of 10-day PAN-treated vs. control animals' GEC foot processes by EM is shown in Fig. 2. In the normal animals the GEC foot processes were tall and narrow and evenly arranged along the

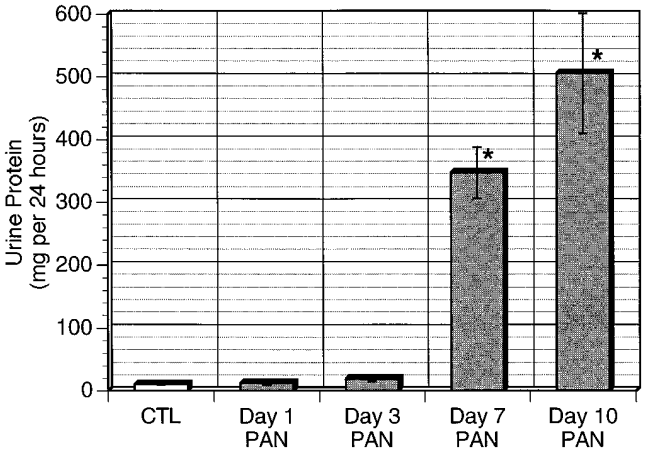

Figure 1. 24 h proteinuria after PAN treatment. Measurement of mean total urine protein (mg) in 24-h urine collections from rats at multiple time points after either a single intraperitoneal injection of PAN (150 mg/kg) or equal volume of saline. *$P < 0.001$ vs. control ($n = 5$ PAN-treated animals at each time point and 25 control animals).

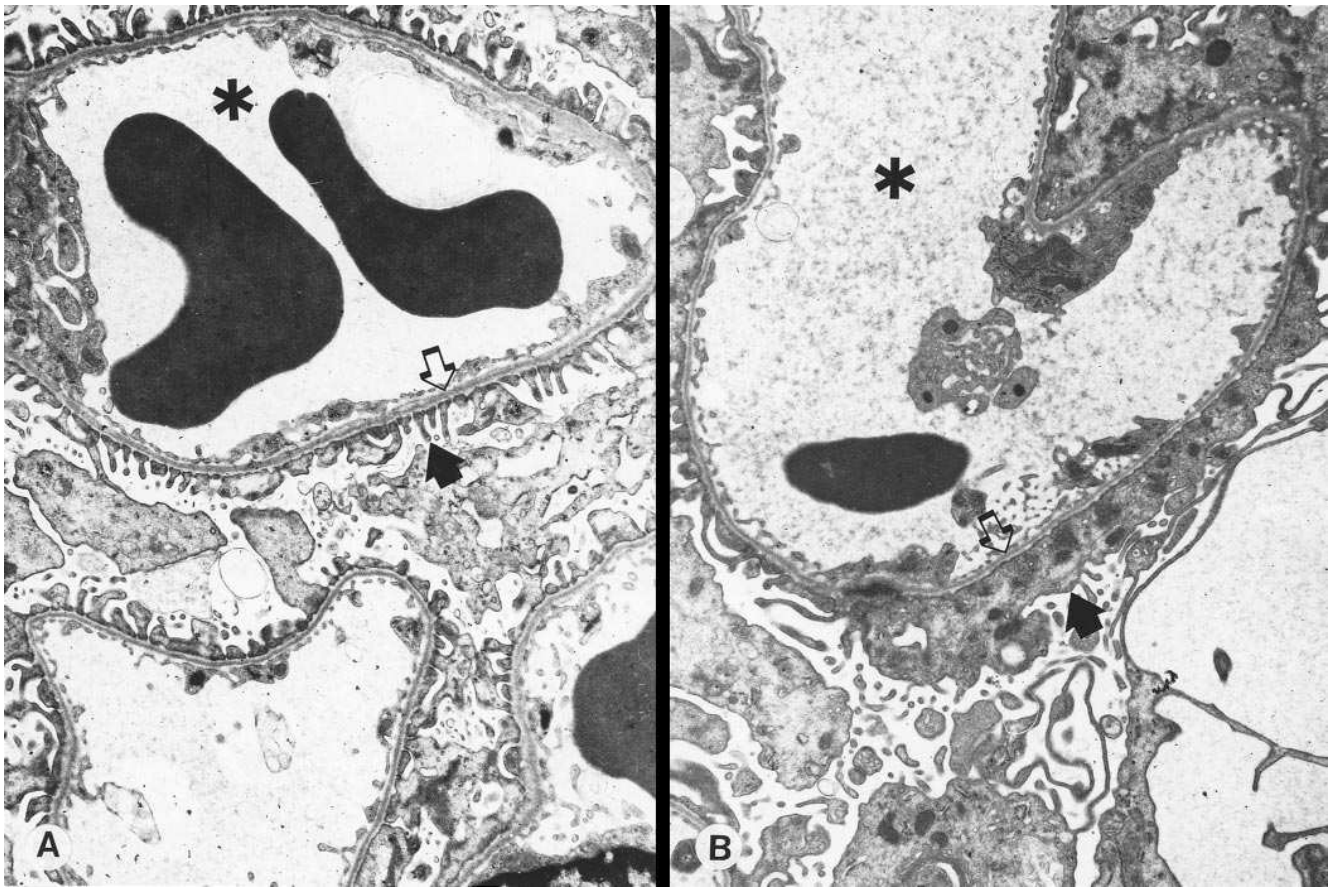

Figure 2. Ultrastructural glomerular changes induced by PAN treatment. Electron microscopic sections from a representative control (*A*) and PAN-treated (*B*) rat glomerulus 10 d after either a single intraperitoneal injection of PAN (150 mg/kg) or equal volume of saline. In *A* the distal GEC foot processes (*solid arrow*) are similar in size and shape and are evenly spaced along the GBM (*open arrow*) which surrounds the glomerular capillary loop (*asterisk*). In contrast, in *B* the GEC foot processes (*solid arrow*) appear spread out along the GBM (*open arrow*), fewer in number, and irregularly shaped. Along much of the GBM they have formed a continuous cytoplasmic sheet. In some areas (not shown) the foot processes have become detached from the underlying GBM. ×5016.

GBM. In contrast, the PAN-treated animals' GEC foot processes had fused into wide cytoplasmic sheets stretched along the GBM, with intermittent detachment of the cytoplasmic sheets from the GBM.

Glomerular hsp27 protein expression

Semi-quantitative confocal microscopy. The expression of hsp27 in representative glomeruli from control and PAN-treated rats 10 d after injection is shown in Fig. 3. In both the control (*A*) and PAN-treated (*B*) sections the staining is distributed in a pattern most consistent with glomerular capillary loop expression, with less intense mesangial, and very little interstitial or tubular staining. Comparison of identical photographic exposures of control vs. PAN-treated glomeruli reveals a marked increase in hsp27 labeling within the diseased animals' glomeruli. In addition, the staining pattern in the PAN-treated animals' glomeruli reveals an apparent consolidation of hsp27 around the glomerular capillary loops. Specificity of the hsp27 mAb for rat hsp27 was confirmed by elimination of glomerular IF staining after preadsorption of the antibody with the hsp27 immunizing peptide (data not shown).

Fig. 4 *A* shows the total glomerular hsp27 labeling during the 10 d after PAN treatment, as analyzed by semi-quantitative confocal IF microscopy. An analysis was performed (in blinded fashion) on 10 randomly selected glomeruli from each of 5 animals (50 glomeruli) for each time period after PAN injection, and from each of 25 animals (250 glomeruli) for the control group. During the course of development of clinical and histologic disease among the PAN-treated animals, there was an increase in glomerular hsp27 IF labeling which was highly significant ($87\pm2\%$, $x\pm$SEM, $P < 0.001$) compared to control animals at 10 d after PAN injection. These increases in IF labeling of glomeruli may not relate in a 1:1 fashion to increases in total glomerular hsp27 protein, but they do permit a relative comparison of glomerular hsp27 between control and diseased animals.

Isoelectric focusing gel analysis. Glomerular hsp27 protein expression was also analyzed using isoelectric focusing gel analysis. This technique provided the ability to quantitate expression of both total glomerular hsp27 and each of the three hsp27 isoforms (unphosphorylated, singly phosphorylated, and doubly phosphorylated) in rat glomeruli. Changes in total glomerular hsp27 expression were quantitated by comparing the sums of the three phosphorylated hsp27 isoform bands for each control and diseased animal and are shown in Fig. 4 *B*. This analysis also revealed a significant ($85\pm25\%$, $x\pm$SEM, $P < 0.05$ vs. control) increase in total glomerular hsp27 expression at 10 d after PAN injection, and confirmed the confocal IF

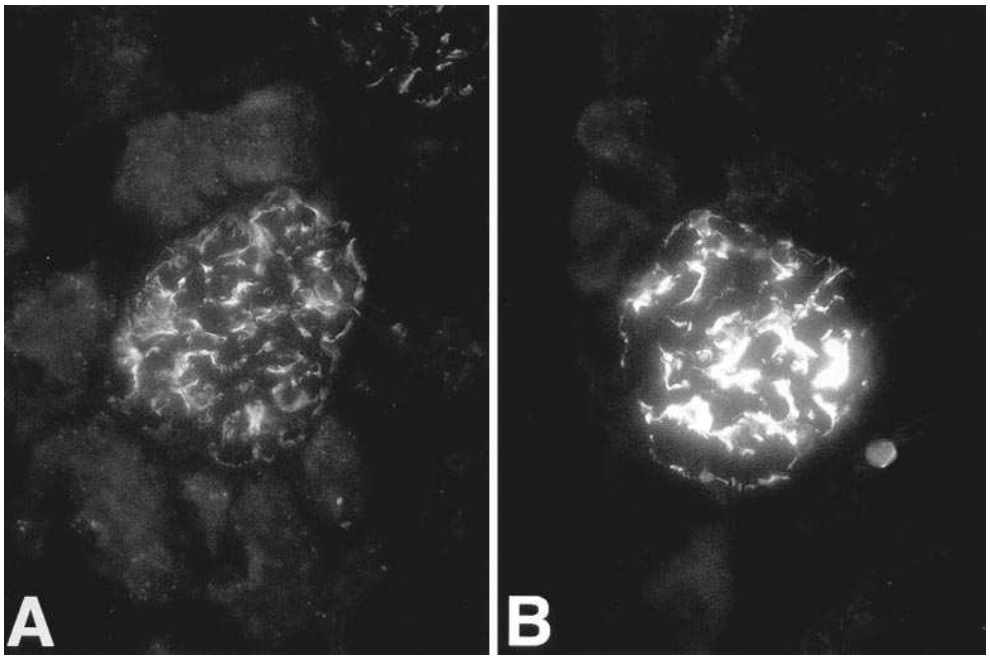

Figure 3. Immunofluorescence staining of glomerular hsp27 in control and PAN-treated rats. Immunofluorescence staining of glomeruli in representative control (*A*) and PAN-treated (*B*) rat kidney sections 10 d after a single intraperitoneal injection of either PAN (150 mg/kg) or equal volume of saline. To demonstrate the relative intensity of staining, exposure times and processing for both photos were identical.

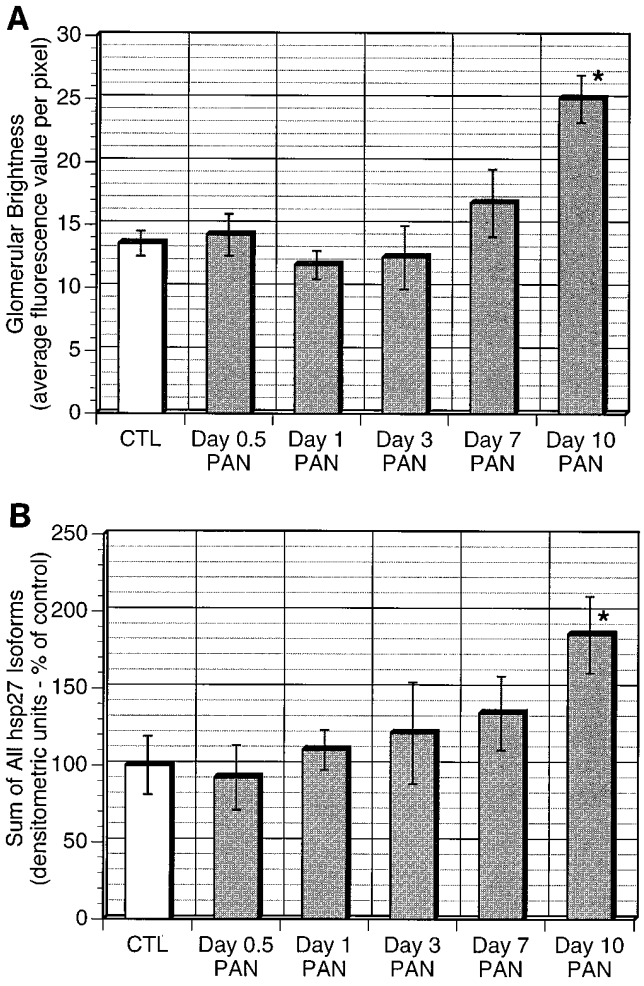

Figure 4. Total glomerular hsp27 after PAN treatment. Glomerular hsp27 protein expression was analyzed at multiple time points following a single intraperitoneal injection of PAN (150 mg/kg) or equal volume of saline (CTL). Measurement of hsp27 expression using semi-quantitative confocal immunofluorescence microscopy (*A*) revealed a significant (87±2%, x±SEM, $P < 0.001$ vs. CTL) increase in glomerular hsp27 labeling during development of nephrotic syndrome ($n = 5$ PAN-treated animals [50 glomeruli] at each time point and 25 control animals [250 glomeruli]). Measurement of total hsp27 expression (the densitometric sum of all 3 detected hsp27 isoforms) from isolated glomeruli by western blotting of isoelectric focusing gels (*B*) also demonstrated a significant (85±25%, x±SEM, $P < 0.05$ vs. CTL) increase in glomerular hsp27 during development of nephrotic syndrome. ($n = 5$ PAN-treated animals at each time point and 25 control animals.)

results. Although increases in band density may not correlate precisely with increases in protein expression, comparison of densitometric results using increasing amounts of glomerular protein revealed a 1:0.88 correlation between protein quantity and densitometric readings, for the amounts of glomerular protein used in these studies (data not shown).

Fig. 5 shows the relative expression of each of the three hsp27 isoforms (unphosphorylated, singly phosphorylated, and doubly phosphorylated) for 25 control animals and 5 PAN-treated animals at each time point after injection, as determined by densitometric analysis of each band. Expression of each of the three phosphorylated hsp27 isoforms increased during the development of nephrotic syndrome (79±21% for the unphosphorylated isoform (*shaded bars*); 80±34% for the singly phosphorylated isoform (*open bars*); and 101±32% for the doubly phosphorylated isoform (*solid bars*); x±SEM). These increases were statistically significant for the unphosphorylated ($P < 0.05$ vs. control) and doubly phosphorylated ($P < 0.05$ vs. control) isoforms, but failed to reach significance for the singly phosphorylated isoform ($0.05 < P < 0.1$ vs. control) due to the large standard errors inherent in using this technique. Subsequent analysis of this increase by paired, two-tailed t test was significant at the $P < 0.05$ level. Analysis of

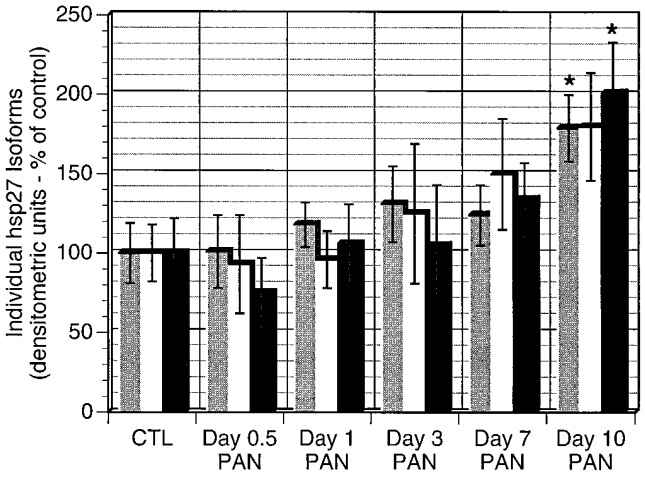

Figure 5. Glomerular expression of each of the three phosphorylated hsp27 isoforms after PAN treatment. Western blots of mini-isoelectric focusing gels from isolated glomeruli were analyzed at multiple time points following a single intraperitoneal injection of PAN (150 mg/kg) or equal volume of saline (CTL). Densitometric analysis of each band at each time point revealed significant increases in the expression of the unphosphorylated isoform (shaded bars) (79±21%, x±SEM, $P < 0.05$ vs. control) and the doubly phosphorylated isoform (black bars) (101±32%, $P < 0.05$ vs. control) during the development of nephrotic syndrome. The increased expression of the singly phosphorylated isoform (white bars) (80±34%, $0.05 < P < 0.1$ vs. control) failed to reach statistical significance due to the large standard errors inherent in using this technique. ($n = 5$ PAN-treated animals at each time point and 25 control animals.)

changes in the relative proportions of individual isoforms expressed during the development of disease failed to identify any significant changes (data not shown). Since hsp27 phosphorylation is a post-translational modification, these findings suggest that both hsp27 expression and phosphorylation are increased during development of nephrotic syndrome.

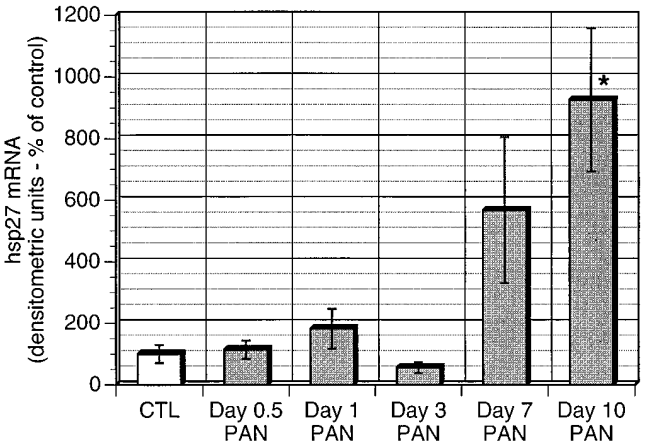

Figure 6. Renal cortical hsp27 mRNA expression after PAN treatment. Renal cortical hsp27 mRNA expression was analyzed at multiple time points after a single intraperitoneal injection of PAN (150 mg/kg) or equal volume of saline (CTL). After normalization of hsp27 expression for RNA loading using 18S rRNA bands from EtBr-stained gels, renal cortical hsp27 mRNA expression increased significantly (826±233%, x±SEM, $P < 0.01$ vs. CTL) by 10 d after PAN injection. ($n = 5$ PAN-treated animals at each time point and 25 control animals.)

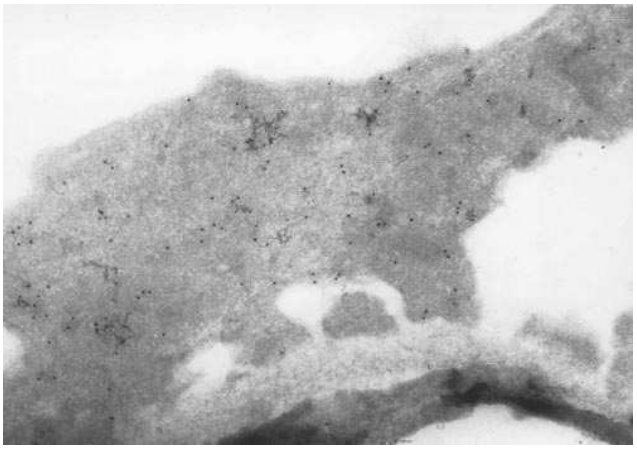

Figure 7. Electron microscopic localization of hsp27 within normal glomerular capillary loops. Subcellular hsp27 localization was performed in normal rat kidney tissue using immunogold labeling. Gold labeling was seen distributed throughout the GEC, but virtually no endothelial cell labeling was present. Mesangial cell labeling was also negligible (not shown). Control sections prepared in an identical manner, except for replacement of the primary antibody with blocking solution, revealed virtually no gold labeling. ×27,200.

Renal cortical hsp27 mRNA expression

Northern blotting. Fig. 6 shows the results of Northern blot analyses of hsp27 mRNA expression in renal cortex. After standardization of all samples for total RNA loading using 18s rRNA expression, densitometric analysis of hsp27 bands for 25 control animals and 5 PAN-treated animals at each time point revealed a significant increase (826±233%, x±SEM, $P < 0.01$ vs. control) in hsp27 mRNA expression at 10 d after PAN injection.

hsp27 immunoelectron microscopic localization

Immunogold labeling. The results of hsp27 immunogold labeling of normal rat renal cortex are shown in Fig. 7. This representative high magnification (34,000×) photomicrograph of a section of a glomerular capillary loop demonstrates significant hsp27 labeling distributed throughout the GEC. Examination of other areas revealed negligible hsp27 labeling of endothelial or mesangial cells, or of the basement membrane. Control sections prepared in an identical manner, except for replacement of the primary antibody with blocking solution, revealed virtually no gold labeling.

Discussion

The mechanism(s) by which nephrotic syndrome occurs remains one of the most important unanswered questions in nephrology today. Several reports have documented the gross morphologic changes which occur in GECs at the EM level during development of the nephrotic syndrome (11, 27). These changes include cell swelling, retraction and effacement of GEC foot processes resulting in the formation of a diffuse cytoplasmic sheet along the GBM, vacuole formation, occurrence of occluding junctions with displacement of slit diaphragms, and detachment of the GEC from the GBM (10, 24). Relatively little data, however, have been reported on the biochemical or molecular events which occur in GECs in association with these morphologic changes (24, 25, 31), and even less

information has been reported on how these changes might be regulated. From a pathophysiologic perspective it is clear that a variety of pathogenic mechanisms, including immunologic processes, biochemical defects (induced by endogenous or exogenous factors), and hemodynamically induced injury to the glomerulus can induce the nephrotic syndrome (32). Because these various stimuli result in the development of a similar pattern of clinical and histologic features, however, it is likely that there is a final common molecular pathway by which the normal regulation of GEC foot process structure is disturbed during development of the nephrotic syndrome.

The present study initially identified the low molecular weight heat shock protein, hsp27, in the glomerular capillary loops of normal rat kidneys. Heat shock proteins comprise several families of intracellular proteins whose expression are increased after exposure to heat or various metabolic insults. These proteins have been reported to be involved in the folding, assembly, translocation, function, and degradation of intracellular proteins and protein complexes (33–35). Although high molecular weight hsps (e.g., hsps 60, 72, and 90) have been reported to be present in the kidney (36–40), localization of hsp27 to the kidney (normal or diseased) has not been previously reported.

The precise function(s) of hsp27 are not yet known. Suggested functions have included involvement in signal transduction, resistance to thermal and metabolic stress, growth and differentiation, and serving as a molecular chaperone (41–47). Recent reports identified hsp27 as an actin-associated protein (21) which inhibits actin polymerization in vitro (22). Subsequent reports suggest that hsp27 may be a component of a signal transduction pathway that may regulate actin microfilament dynamics and that its actin polymerization-inhibiting activity is related to its state of phosphorylation (23, 48–50). One such signal transduction pathway has now been characterized in a human carcinoma cell line, where it has been demonstrated that hsp27 is phosphorylated as a result of activation of a protein kinase cascade by the cytokine interleukin-1 (51).

Our initial localization of hsp27, an intracellular protein, to the glomerular capillary loop by IF microscopy suggested that it could be expressed in either glomerular endothelial cells, GECs, or in both cell types. Subsequent immunoelectron microscopy has confirmed that glomerular hsp27 is expressed almost exclusively within GECs. This finding in normal kidney, along with the reported regulation of actin polymerization by hsp27, suggest that hsp27 may play a role in the maintenance of normal GEC foot process structure via regulation of actin microfilament structure and dynamics.

Induction of experimental nephrotic syndrome and GEC foot process effacement resulted in both increased expression and enhanced phosphorylation of glomerular hsp27. In light of recent reports that the regulation of actin polymerization by hsp27 is dependent on hsp27 phosphorylation (23, 48–50), these results further support our hypothesis that alterations in glomerular hsp27 expression and phosphorylation may have an important role in regulating pathophysiologic changes in actin microfilaments within GECs during development of GEC foot process effacement and clinical nephrotic syndrome.

In previous reports, expression of unphosphorylated hsp27 has been associated with inhibition of actin polymerization, while phosphorylation of hsp27 has diminished its actin polymerization-inhibiting activity (23). Within this context, glomerular hsp27 expression in the normal state may reflect the dynamic regulation of the balance between actin polymerization and depolymerization within the GEC necessary to maintain its normal shape and function. A pathophysiologic stimulus capable of inducing the nephrotic syndrome might involve hsp27 in any of three manners: (*a*) The stimulus might induce hsp27 expression and phosphorylation within GECs, resulting in disruption of the delicate balance between actin polymerization and depolymerization within the foot processes. Such an imbalance in cytoskeletal regulation might further result in loss of normal GEC foot process structure and function, culminating in GEC foot process effacement and development of proteinuria. In this scenario hsp27 would clearly have a pathophysiologic role in the development of nephrotic syndrome. (*b*) Alternatively, the stimulus might produce GEC foot process effacement directly, with the induction of hsp27 expression and phosphorylation representing a specific response by the GECs to the marked alterations in actin dynamics associated with foot process effacement. In this scenario hsp27 would have a specific protective or reparative role in the GEC's response to and/or recovery from the cellular stress. In support of this are several reports where transfection of hsp27 cDNA into various cell types resulted in dramatically increased resistance to thermal and oxidative stresses (45, 46, 52, 53) (W. Wu, and M.J. Welsh, manuscript submitted for publication). (*c*) Finally, the stimulus might produce GEC foot process effacement directly, but with the induction of hsp27 expression and phosphorylation representing a potentially nonspecific stress response of the GECs, unrelated to altered actin dynamics. Of these three possibilities our data most strongly supports the second, since significant elevations of hsp27 expression and phosphorylation were not seen until after the development of massive proteinuria and GEC foot process effacement.

In summary, the present study has demonstrated significant expression of the low molecular weight heat shock protein, hsp27, in GECs within the glomerular capillary loops of normal rats. Induction of experimental nephrotic syndrome resulted in both increased expression and enhanced phosphorylation of glomerular hsp27 in association with development of GEC foot process effacement and massive proteinuria. In light of the reported regulation of actin polymerization by hsp27, these findings suggest that hsp27 may regulate GEC foot process actin polymerization, and thus have an important role both in the maintenance of normal foot process structure and in the pathophysiologic cytoskeletal changes which occur in these processes during development of the nephrotic syndrome.

Acknowledgments

The authors would like to thank Roger C. Wiggins and William Wu for their critical reviews of this manuscript, and for their helpful discussions and advice during the development of this work. Our thanks also to Lisa Riggs and Robin Kunkel for their help with the IF and EM tissue preparation and analysis. Lisa Riggs is supported by a George M. O'Brien Renal Center Grant from the U.S. Public Health Service.

This work was supported in part by National Institutes of Health grant R01 ES06265 and by Reproductive Hazards in the Workplace, Home, Community, and Environment Research grant 15-FY94-0705 from the March of Dimes Birth Defects Foundation to M.J. Welsh. The Laboratory Animal Core was supported by NIH grant P30 HD18258.

References

1. Hoyer, J.R. 1982. Idiopathic nephrotic syndrome with minimal changes. *Contemp. Issues Nephrol.* 9:145–170.

2. Mavichak, V., and J.H. Dirks. 1988. Pathophysiology of the nephrotic syndrome: mechanisms of edema. *In* The Nephrotic Syndrome. J.S. Cameron, and R.J. Glassock, editors. Marcel Dekker, Inc., New York. 251–283.

3. Levin, M., P. Gascoine, M.W. Turner, and T.M. Barratt. 1989. A highly cationic protein in plasma and urine of children with steroid-responsive nephrotic syndrome. *Kidney Int.* 36:867–877.

4. Schnaper, H.W., and T.M. Aune. 1985. Identification of the lymphokine soluble immune response suppressor in urine of nephrotic children. *J. Clin. Invest.* 76:341–349.

5. Schnaper, H.W., and T.M. Aune. 1987. Steroid-sensitive mechanism of soluble immune response suppressor production in steroid-responsive nephrotic syndrome. *J. Clin. Invest.* 79:257–264.

6. Moorthy, A.V., S.W. Zimmerman, and P.M. Burkholder. 1976. Inhibition of lymphocyte blastogenesis by plasma of patients with minimal-change nephrotic syndrome. *Lancet.* 1:1160–1162.

7. Sobel, A.T., A.I. Branellec, C.J. Blanc, and G.A. Lagrue. 1977. Physicochemical characterization of a vascular permeability factor produced by Con-A–stimulated human lymphocytes. *J. Immunol.* 119:1230–1234.

8. Lagrue, G., J. Laurent, and G. Rostoker. 1989. Food allergy and idiopathic nephrotic syndrome. *Kidney Int*. 36:S147–S151.

9. Koyama, A., M. Fujisaki, M. Kobayashi, M. Igarashi, and M. Narita. 1991. A glomerular permeability factor produced by human T cell hybridomas. *Kidney Int*. 40:453–460.

10. Caulfield, J.P., J.J. Reid, and M.G. Farquhar. 1976. Alterations of the glomerular epithelium in acute aminonucleoside nephrosis. Evidence for formation of occluding junctions and epithelial cell detachment. *Lab Invest*. 34:43–59.

11. Ryan, G.P., and M.J. Karnovsky. 1975. An ultrastructural study of the mechanisms of proteinuria in aminonucleoside nephrosis. *Kidney Int*. 8:219–232.

12. Klein, D.J., P.J. Dehnel, T.R. Oegema, and D.M. Brown. 1984. Alterations in proteoglycan metabolism in the nephrotic syndrome induced by the aminonucleoside of puromycin. *Lab. Invest*. 50:543–551.

13. Hoyer, J.R., J. Ratte, A.H. Potter, and A.F. Michael. 1972. Transfer of aminonucleoside nephrosis by renal transplantation. *J. Clin. Invest*. 51:2777–2780.

14. Nakamura, T., I. Ebihara, I. Shirato, Y. Tomino, and H. Koide. 1991. Modulation of basement membrane component gene expression in glomeruli of aminonucleoside nephrosis. *Lab. Invest*. 64:640–647.

15. Bakker, W.W., and W.H. van Luijk. 1989. Do circulating factors play a role in the pathogenesis of minimal change nephrotic syndrome? *Pediatr. Nephrol.* 3:341–349.

16. Silva, F.G., and R.J. Hogg. 1989. Minimal change nephrotic syndrome-focal sclerosis complex (including IgM nephropathy and diffuse mesangial hypercellularity). *In* Renal Pathology. Vol. 1. Tisher C.C., and B.B.M., editors. J.B. Lippencott Company, Philadelphia, PA. 275–280.

17. Farquhar, M.G., R.L. Vernier, and R.A. Good. 1957. An electron microscopic study of the glomerulus in nephrosis, glomerulonephritis and lupus erythematosus. *J. Exp. Med*. 106:649–660.

18. Whiteside, C., K. Prutis, R. Cameron, and J. Thompson. 1989. Glomerular epithelial detachment, not reduced charge density, correlates with proteinuria in adriamycin and puromycin nephrosis. *Lab. Invest*. 61:650–660.

19. Vasmant, D., M. Maurice, and G. Feldmann. 1984. Cytoskeletal ultrastructure of podocytes and glomerular endothelial cells in man and in the rat. *Anat. Rec*. 210:17–24.

20. Andrews, P.M., and S.B. Bates. 1984. Filamentous actin bundles in the kidney. *Anat. Rec*. 210:1–9.

21. Miron, T., M. Wilchek, and B. Geiger. 1988. Characterization of an inhibitor of actin polymerization in vinculin-rich fraction of turkey gizzard smooth muscle. *Eur. J. Biochem*. 178:543–553.

22. Miron, T., M. Wilchek, and B. Geiger. 1991. A 25 kD inhibitor of actin polymerization is a low molecular mass heat shock protein. *J. Cell Biol*. 114: 255–261.

23. Benndorf, R., K. Hayeb, S. Ryazantsev, M. Wieske, J. Behlke, and G. Lutsch. 1994. Phosphorylation and supramolecular organization of murine small heat shock protein HSP25 abolish its actin polymerization-inhibiting activity. *J. Biol. Chem*. 269:20780–20784.

24. Ito, K., Y.C. Ger, and S. Kawamura. 1986. Actin filament alterations in glomerular epithelial cells of adriamycin-induced nephrotic rats. *Acta. Pathol. Jpn*. 36 (2):253–260.

25. Whiteside, C.I., R. Cameron, S. Munk, and J. Levy. 1993. Podocytic cytoskeletal disaggregation and basement-membrane detachment in puromycin aminonucleoside nephrosis. *Am. J. Pathol*. 142:1641–1653.

26. Lachapelle, M., and M. Bendayan. 1991. Contractile proteins in podocytes: Immunochemical localization of actin and alpha-actinin in normal and nephrotic rat kidneys. *Virchows Arch. B Cell Pathol*. 60:105–111.

27. Vernier, R.L., B.W. Papermaster, and R.A. Good. 1958. Aminonucleoside nephrosis. I. Electron microscopic study of the renal lesion in rats. *J. Exp. Med*. 109:115–126.

28. Kreisberg, J.I., R.L. Hoover, and M.J. Karnovsky. 1978. Isolation and characterization of rat glomerular epithelial cells in vitro. *Kidney Int*. 14:21–30.

29. Bitar, K.N., M.S. Kaminski, N. Hailat, K.B. Cease, and J.R. Strahler. 1991. HSP27 is a mediator of sustained smooth muscle contraction in response to bombesin. *Biochem. Biophys. Res. Commun*. 181:1192–1200.

30. Selden, R.F. 1992. Analysis of RNA by northern hybridization. *In* Current Protocols in Molecular Biology. Vol. 1. F.M. Ausubel, R. Brent, R.E. Kingston, D.D. Moore, J.G. Seidmen, J.A. Smith, and K. Struhl, editors. John Wiley & Sons, New York. 4.9.1–4.9.8.

31. Sharma, R., H.B. Lovell, T.B. Wiegmann, and V.J. Savin. 1992. Vasoactive substances induce cytoskeletal changes in cultured rat glomerular epithelial cells. *J. Am. Soc. Nephrol*. 3:1131–1138.

32. Glassock, R.J. 1988. Pathogenesis of the nephrotic syndrome. *In* The Nephrotic Syndrome. J.S. Cameron, and R.J. Glassock, editors. Marcel Dekker, Inc., New York. 163–192.

33. Lindquist, S., and E.A. Graig. 1988. The heat shock proteins. *Annu. Rev. Genet*. 22:631–677.

34. Rothman, J.E. 1989. Polypeptide chain binding proteins: Catalysts of protein folding and related processes in cells. *Cell*. 59:591–601.

35. Welch, W.J. 1992. Mammalian stress response: Cell physiology, structure/function of stress proteins, and implications for medicine and disease. *Physiol. Rev*. 72:1063–1081.

36. Ross, W.R., W.S. Bertrand, and A.R. Morrison. 1992. Identification of a processed protein related to the human chaperonins (hsp60) protein in mammalian kidney. *Biochem. Biophys. Res. Commun*. 185 (2):683–687.

37. Wakui, H., H. Itoh, R. Tashima, Y. Nakamoto, and A.B. Miura. 1992. Purification of a mature form of 60 kDa heat-shock protein (chaperonin homolog) from porcine kidney and its partial amino acid sequence. *Int. J. Biochem*. 24 (9):1507–1510.

38. Komatsuda, A., H. Wakui, H. Imai, Y. Nakamoto, A.B. Miura, H. Itoh, and Y. Tashima. 1992. Renal localization of the constitutive 73-kDa heat-shock protein in normal and PAN rats. *Kidney Int*. 41 (5):1204–1212.

39. Emami, A., J.H. Schwartz, and S.C. Borkan. 1991. Transient ischemia or heat stress induces a cytoprotectant protein in rat kidney. *Am. J. Physiol*. 260: F479–485.

40. Matsubara, O., T. Kasuga, F. Marumo, H. Itoh, and Y. Tashima. 1990. Localization of the 90-kDa heat shock protein in the kidney. *Kidney Int.* 38: 830–834.

41. Ciocca, D.R., S. Oesterreich, G.C. Chamness, W.L. McGuire, and S.A. W. Fuqua. 1993. Biological and clinical implications of heat shock protein 27 000 (Hsp27): a review. *J. Natl. Cancer Inst.* 85:1558–1570.

42. Jakob, U., M. Gaestel, K. Engel, and J. Buchner. 1993. Small heat shock proteins are molecular chaperones. *J. Biol. Chem*. 268:1517–1520.

43. Lavoie, J.N., G. Gingras-Breton, R.M. Tanguay, and J. Landry. 1993. Induction of Chinese hamster hsp27 gene expression in mouse cells confers resistance to heat shock. *J. Biol. Chem*. 268:3420–3429.

44. Mehlen, P., X. Preville, P. Chareyron, J. Briolay, R. Klemenz, and A.P. Arrigo. 1995. Constitutive expression of human hsp27, Drosophila hsp27 or human αB-Crystallin confers resistance to TNF- and oxidative stress-induced cytotoxicity in stably transfected murine L929 fibroblasts. *J. Immunol*. 154:363–374.

45. Huot, J., G. Roy, H. Lambert, P. Chretien, and J. Landry. 1991. Increased survival after treatments with anticancer agents of Chinese hamster cells expressing the human M_r 27,000 heat shock protein. *Cancer Res*. 51:5245–5252.

46. Landry, J., P. Chretien, H. Lambert, E. Hickey, and L.A. Weber. 1989. Heat shock resistance conferred by expression of the human HSP27 gene in rodent cells. *J. Cell Biol*. 109:7–15.

47. Arrigo, A.P., and J. Landry. 1994. Expression and function of the low-molecular-weight heat shock proteins. *In* The Biology of Heat Shock Proteins and Molecular Chaperones. R.I. Morimoto, A. Tissieres, and C. Georgopoulos, editors. Cold Spring Harbor Laboratory Press, Plainview. 335–373.

48. Lavoie, J., E. Hickey, L.A. Weber, and J. Landry. 1993. Modulation of actin microfilament dynamics and fluid phase pinocytosis by phosphorylation of heat shock protein 27. *J Biol. Chem*. 268:24210–24214.

49. Lavoie, J.N., H. Lambert, E. Hickey, L.A. Weber, and J. Landry. 1995. Modulation of cellular thermoresistance and actin filament stability accompanies phosphorylation-induced changes in the oligomeric structure of heat shock protein 27. *Mol. Cell Biol*. 15:505–516.

50. Huot, J., F. Houle, D.R. Spitz, and J. Landry. 1996. HSP27 phosphorylation-mediated resistance against actin fragmentation and cell death induced by oxidative stress. *Cancer Res*. 56:273–279.

51. Freshney, N.W., L. Rawlinson, F. Guesdon, E. Jones, S. Cowley, J. Hsuan, and J. Saklatvala. 1994. Interleukin-1 activates a novel protein kinase cascade that results in the phosphorylation of hsp27. *Cell*. 78:1039–1049.

52. Rollet, E., J.N. Lavoie, J. Landry, and R.M. Tanguay. 1992. Expression of Drosophila's 27kD heat shock protein into rodent cells confers thermal resistance. *Biochem. Biophys. Res. Commun*. 185:116–120.

53. Mehlen, P., J. Briolay, L. Smith, C. Diaz-Latoud, N. Fabre, D. Pauli, and A.P. Arrigo. 1993. Analysis of the resistance to heat and hydrogen peroxide stresses in COS cells transiently expressing wild type or deletion mutants of the Drosophila 27-kD heat shock protein. *Eur. J. Biochem*. 215:277–284.